HHS Public Access

Author manuscript

Biomacromolecules. Author manuscript; available in PMC 2023 April 11.

Published in final edited form as:

Biomacromolecules. 2022 April 11; 23(4): 1703–1712. doi:10.1021/acs.biomac.1c01635.

Theranostic copolymers neutralize reactive oxygen species and lipid peroxidation products for combined treatment of traumatic brain injury

Aaron Priester[1], **Richard Waters**[1], **Ashleigh Abbott**[1], **Krista Hilmas**[1], **Klaus Woelk**[1], **Hunter A. Miller**[2], **Aria W. Tarudji**[2], **Connor C. Gee**[2], **Brandon McDonald**[2], **Forrest M. Kievit**[2], **Anthony J. Convertine**[1,*]

[1]Department of Material Science and Engineering, Missouri University of Science and Technology, Rolla, MO, USA

[2]Department of Biological Systems Engineering, University of Nebraska-Lincoln, NE, 68583-0900, USA

Abstract

Traumatic brain injury (TBI) results in the generation of reactive oxygen species (ROS) and lipid peroxidation product (LPOx) including acrolein and 4-hydroxynonenal (4HNE). The presence of these biochemical derangements results in neurodegeneration during the secondary phase of the injury. The ability to rapidly neutralize multiple species could significantly improve outcomes for TBI patients. However, difficulty in creating therapies that target multiple biochemical derangements simultaneously has greatly limited therapeutic efficacy. Therefore, our goal was to design a material that could rapidly bind and neutralize both ROS and LPOx following TBI. To do this, a series of thiol-functionalized biocompatible copolymers based on lipoic acid methacrylate (LIPOMA) and polyethylene glycol monomethyl ether methacrylate (FW ~ 950 Da) (O950) were prepared. A polymerizable gadolinium-DOTA methacrylate monomer (Gd-MA) was also synthesized starting from cyclen to facilitate direct magnetic resonance imaging (MRI) and in vivo tracking of accumulation. These neuroprotective copolymers (NPCs) were shown to rapidly and effectively neutralize both ROS and LPOx. Horseradish peroxidase (HRPO) absorbance assays showed that the NPCs efficiently neutralized H_2O_2 while R-phycoerythrin protection assays demonstrated their ability to protect the fluorescent protein from oxidative damage. ^{1}H NMR studies indicated the thiol-functional NPCs rapidly form covalent bonds with acrolein, efficiently

*Correspondence should be addressed to: convertinea@mst.edu.

Author Contributions

The manuscript was written through contributions of all authors. All authors have given approval to the final version of the manuscript.

Supporting Information. The Supporting Information is available free of charge at: *Synthesis of mon(LIPOMA) from α-Lipoic Acid, Synthesis of mon(Gd DOTA),* TRI-BOC synthesis, SMA Cl synthesis, BOC DOTA synthesis, Gd DOTA synthesis, *Synthesis of poly(LIPOMA-co-0950) series, Synthesis of poly(O950), Synthesis of poly((LIPOMA-co-0950)-b-(O950-co-GdMA)), Reduction of poly(Lipoma-co-0950) with sodium borohydride, Reduced poly(LIPOMA-co-O950) thiol quantification, Quantifying the effect of reduced poly(LIPOMA-co-O950) series polymers on H_2O_2 neutralization by HRPO Assay Method, Quantifying the effect of poly(LIPOMA-co-O950) series polymers on Cu free radical neutralization using R-phycoerythrin fluorescent protein assay, Quantifying the effect of poly(LIPOMA-co-O950) series polymers on acrolein neutralization using NMR, Quantifying the effect of reduced LP20 copolymer on SH-SY5Y cell viability against H_2O_2 and acrolein,* Controlled Cortical Impact Mouse Model of TBI, In vivo Dynamic Contrast-Enhanced Magnetic Resonance Imaging (DCE-MRI), Dihydroethidium Histological Analysis, Molecular Weights and Polydispersities of poly(LIPOMA-co-O950) series, *Dynamic Light Scattering for particle size determination of poly(LIPOMA-co-O950) series*, 1H NMR and 13C NMR spectra for LIPOMA monomer

removing it from solution. In vitro cell studies with SH-SY5Y-differentiated neurons showed that NPCs provide unique protection against toxic concentrations of both H_2O_2 and acrolein. NPCs rapidly accumulate and are retained in injured brain in controlled cortical impact mice and reduce post-traumatic oxidative stress. Therefore, these materials show promise for improved target engagement of multiple biochemical derangements in hopes of improving TBI therapeutic outcomes.

Keywords

Traumatic brain injury; Reactive oxygen species; Lipid peroxidation product; RAFT polymerization; Theranostic; Antioxidant; polymer

Introduction

Traumatic brain injury (TBI) is a major cause of disability and death among children and young adults. Damage from a TBI occurs in two separate phases which consist of the initial brain trauma and a secondary phase.[1,2] During the secondary phase, reperfusion injury, delayed cortical edema, and blood−brain barrier breakdown can result in the release of ROS, calcium imbalances, and the production of highly reactive lipid peroxidation products.[3,4] During the secondary phase, which progresses over the course of days to weeks, this release of ROS, calcium, and lipid peroxidation products leads to increased cytokine and chemokine expression the formation of chronically reactive astrocytes and activated microglia. [5] These biochemical and cellular cascades lead to neural degeneration and progression of tissue damage into other regions of the brain. As a result, many of the lifelong problems that arise following a TBI can at least partially be attributed mechanisms that occur following the initial brain trauma.[6] Current therapies provide only palliative support for TBI patients highlighting the need for new therapeutic agents that are capable of minimizing neurodegeneration during the secondary phase of the injury. [7–10] Several antioxidant therapies have been investigated including PEG-conjugated superoxide dismutase,[11] PEG conjugated catalase, [12] tirilazad, [13] as well as combinations of these agents. Although these antioxidant materials have shown promise in preclinical studies they have failed to improve patient outcome in large clinical studies.

These failed clinical trials stem from numerous drawbacks of current therapies, which include (1) poor delivery into the brain leading to minimal target engagement, (2) incomplete understanding of the disease process leading to suboptimal patient selection, and (3) effectiveness against only one of many therapeutic targets leading to reduced treatment efficacy. As a result, there is a critical need to develop new therapies that are capable of improved brain delivery, robust efficacy against a broad patient population, and the ability to neutralize multiple reactive species associated with the secondary phase of TBI. Such therapies could provide substantial long-term physical, behavioral, and psychosocial benefit for individuals that have sustained a TBI.

Previously, we detailed the development of oxygen reactive polymers (ORPs) and antioxidant nanoparticles that are able to act as both a diagnostic MRI contrast agent and a therapeutic ROS sponge.[14–16] These ORPs, which were prepared by reversible addition-

fragmentation chain transfer (RAFT) polymerization, contain thio-ether residues as the ROS scavenging agent and O950 residues to increase circulation half-life and biocompatibility. Gadolinium contrast agents for MRI analysis were then added post polymerization. These materials were shown to effectively accumulate in damaged brain and reduce histological measures of secondary injury in a controlled cortical impact (CCI) mouse model of TBI. Thiols are another class of antioxidant sulfur compound that rapidly react with free radicals.[17] Additionally, thiols also readily react with electron deficient alkenes via Thiol-Michael addition reactions. [18] The result of this reaction is the formation thioether linkage and the conversion of the highly reactive alkene into an alkane. In these studies, we describe the development of a new series of theranostic polymers that contain thiol residues that are capable of neutralizing both ROS and LPOx.

Results and Discussion

In these studies, our objective was to develop NPCs that can efficiently neutralize both ROS as well as LPOx. In order to accomplish this objective, a series of hydrophilic copolymers containing thiol residues derived from lipoic acid (LA) were synthesized. LA is an endogenous organosulfur compound that is an essential cofactor for several mitochondrial enzymes.[19] Both LA and dihydrolipoic acid (DHLA) are capable of scavenging •OH radicals, but only DHLA is capable of scavenging superoxide radical anions suggesting that DHLA is an excellent antioxidant. [20] LA was selected as the thiol source as this compound: 1) contains a carboxylic acid with which to attach the methacrylate group, 2) is commercially available and inexpensive, and 3) contains two sulfhydryl residues as a disulfide group.

The latter point is necessary for subsequent polymerization of the monomer as free thiol groups efficiently inhibit free radical polymerizations. LA was first converted into a methacrylate monomer (LIPOMA) via carbodiimide mediated esterification with 2-hydroxyethyl methacrylate. LIPOMA was then copolymerized with PEG methacrylate (FW ~ 950 Da) (O950) to prepare a series of neuroprotective copolymers (NPCs). Our previous studies have shown that the large PEG macromonomer can be used to prepare biocompatible copolymers with favorable PK/biodistribution profiles.[21–23]

The LIPOMA containing NPCs were then reduced with sodium borohydride to yield two thiol residues per mole of LIPOMA comonomer. Our hypothesis here was that the thiol groups could serve two neuroprotective functions by both rapidly neutralizing ROS and effectively forming covalent bonds with LPOx via thiol-Michael reactions. RAFT polymerization methodology was employed in order to yield copolymers with controlled molecular weights and narrow molar mass dispersities (Đ). To evaluate the aqueous morphology of the NPCs, a series of polymers with increasing molar feed ratios of the hydrophobic LIPOMA comonomer were synthesized. For all copolymerizations, the initial monomer to chain transfer agent ratio ($[M]_o$:$[CTA]_o$) and initial chain transfer agent to initiator ratio ($[CTA]_o$:$[I]_o$) were held constant at 25 and 20, respectively. These ratios were selected in order to yield copolymers that were below the renal clearance molecular weight. Additionally, a 20 wt% poly(LIPOMA-co-O950) macro CTA was co-blocked with GdMA (contrast agent) and O950 for MRI studies (Scheme 1).

As can be seen in Table 1, a series of copolymers with compositions ranging from 0 to 50 wt. % LIPOMA were prepared.

These materials displayed relatively narrow molar mass dispersities and molecular weights that were generally consistent with theory. For example, NPC 3 with an initial LIPOMA feed percentage of 20 wt. % was determined to have a molecular weight and molar mass dispersity of 26 700 Da and 1.25 respectively. The molecular weight values compare favorably with the theoretical value of 17400 Da with deviations likely arising from the use of polymethyl methacrylate standards. Representative procedures for the synthesis, purification, and characterization of these materials can be found in supplementary information. Analysis of the NPC thiol content was then quantified using Ellman's assay. Here fair agreement between the experimental thiol concentration relative to the theoretical values based on LIPOMA content were observed (SI Figure 6). For example, NPC 3 with a LIPOMA concentration of 20 wt. % was found to contain 0.0008 moles of sulfhydryl groups per g of polymer compared to maximum theoretical sulfhydryl concentration 0.0013 moles per g of polymer for this composition. Here steric constrains likely reduced the ability of Ellman's reagent to place bulky 2-nitro-5-thiobenzoate groups on thiol groups at both carbon 6 and nearby carbon 8. To streamline NPC synthesis, one-pot conditions were then developed in which disulfide reductions were conducted directly in the polymerization medium without the intervening purification steps. Because all polymerizations achieved greater than 99.9 % monomer conversion it was hypothesized that an atom efficient one-pot procedure could be established without noticeable differences in reduction efficiency. Indeed, GPC analysis combined with thiol quantification via Ellman's assay confirmed the viability of the one-pot procedure. Particle sizes were then determined for the NPCs in pH 7.4 phosphate buffered saline (PBS) via dynamic light scattering (DLS). These studies showed that NPCs with up to 20 wt. % have sizes that are consistent with molecularly dissolved unimers (e.g. $D_H < 10$ nm) while higher LIPOMA feed ratios showed larger particle sizes suggesting the formation of nanoparticles ($D_H > 10$ nm) (Table I).

To quantify the ability of the NPCs to neutralize ROS, a simple high-throughput assay based on the HRP-mediated oxidation of phenol red in the presence of H_2O_2 was conducted. Oxidation of phenol red by H_2O_2 in the presence of HRP yields a deep purple color with a high absorbance at 610 nm. This assay provides a convenient method by which NPC antioxidant activity can be monitored simply by following the absorbance of phenol red at 610 nm. As can be seen in Figure 1a, all LIPOMA containing copolymers demonstrated a concentration-dependent ability to reduce the oxidation of phenol red by HRP-H_2O_2.

As expected, the poly(O950) negative control polymer lacking LIPOMA residues showed no ability to prevent the oxidation of phenol red. In contrast, the NPC 2 and 3, which contain 10 and 20 wt.% LIPOMA respectively, reduced the absorbance at 610 nm by 85 % and 95 % respectively at a copolymer concentration of 10 mg mL^{-1}. Interestingly, copolymers containing 30 and 40 wt. % LIPOMA were less efficient at reducing phenol red oxidation than copolymers containing 10 and 20 wt. % LIPOMA. Here NPCs 4 and 5(containing 30 and 40 wt. % LIPOMA) reduced phenol red oxidation by 80% and 70 % respectively relative to polymer free samples. While all NPCs showed potent antioxidant behavior in this assay, these results suggest that copolymers containing higher concentrations of the

hydrophobic LIPOMA comonomer may be forming self-assembled structures that are less accessible to the oxidizer. Based on these results, the 20 wt. % copolymer (NPC 3) was selected for all further studies. We next evaluated the antioxidant ability of NPC 3 as a function of time by preincubating the copolymer with H_2O_2 for different periods of time prior to the addition of phenol red. As can be seen in Figure 1b, the copolymer shows a clear concentration-dependent ability to reduce the absorbance phenol red oxidation. Also evident from this plot is that the antioxidant properties of this copolymer are not especially time-dependent with copolymers pre-incubated with H_2O_2 for 4 hours prior to the introduction of phenol red showing comparable values to those preincubated for only 1 minute. This result is encouraging as it suggests that the copolymers could provide immediate ROS protection following a TBI.

To further confirm the ability of NPC 3 to protect against ROS mediated damage we next conducted an assay using the fluorescent protein R-phycoerythrin (RPE). This assay is based on the high sensitivity of RPE to ROS mediated damage, where a rapid and complete reduction in fluorescence is observed when the protein is incubated with a range of oxidizing agents. In this study, free radicals were generated by mixing ascorbic acid with Cu^{2+} salts. Although ascorbic acid is typically considered an antioxidant, it can also undergo a Fenton reaction with copper ions resulting in the generation of free radicals. The resultant free radicals efficiently oxidize R-phycoerythrin resulting in a rapid reduction fluorescence. NPC 3 mediated ROS neutralization should protect the protein from oxidation thus preserving its fluorescent properties. Shown in Figure 1c are fluorescence values at 575 nm for R-phycoerythrin incubated with NPC 3 at a range of thiol / Cu^{2+} concentrations for incubation times of 15 and 30 minutes. Here NPC 3 showed concentration-dependent preservation of RPE fluorescence with thiol / Cu^{2+} ratios equal of 1.79 or greater providing complete protection. As the thiol / Cu^{2+} ratio is lowered below unity, a progressive loss in RPE fluorescence is observed. For example, a thiol / Cu^{2+} ratio of 0.9 yields RPE fluorescence values of 79% and 72% at 15 and 30 minutes respectively relative to Cu^{2+} free controls. In contrast, the control polymer (poly(O950), NPC 1) shows a rapid time-dependent decrease in fluorescence that is nearly identical to decreases observed for RPE plus oxidizer alone samples (Figure 1d). These results taken together provide direct evidence that NPC 3 is able to protect the ROS sensitive proteins from oxidative damage.

Having established the ability of NPC 3 to protect against ROS mediated damage we next evaluated at this material to neutralize LPOx products by reacting with these species. The electron deficient double bonds of LPOx were hypothesized to undergo thiol-Michael reactions with the thiol-functional copolymer. In order provide support for this hypothesis, the reaction between acrolein and NPC 3 was monitored directly in D_2O by ^1H NMR. Because of the highly unstable nature of acrolein, this compound was generated immediately prior to these studies by acid-mediated hydrolysis of acrolein diethyl acetal. Cleavage of the acetal group under acidic conditions proceeds rapidly generating the aldehyde group and two molar equivalents of ethanol. The stock solution of acrolein was then diluted into phosphate buffered D_2O at pH 7.4. In order to compare between samples, the vinyl and aldehyde resonances were normalized to the ethanol methylene resonance ($HO\mathbf{CH_2}CH_3$) at 1.0 – 1.5 ppm (not shown). The results of these studies can be seen in Figures 1e and 1f,

where the acrolein vinyl resonances located around 7.5 ppm are clearly visible at a thiol to acrolein molar ratio of 0 (no copolymer added). Also visible is the acrolein aldehyde proton located around 11 ppm which changes shape but remains roughly constant in area upon reaction with the copolymer. In contrast, the acrolein vinyl resonances, which are converted into aliphatic thiol-ether groups upon reaction with sulfhydryl groups, showed a progressive reduction in area upon incubation with increasing sulfhydryl/acrolein ratios. Complete disappearance of the acrolein vinyl resonance was observed for the reduced copolymer at a thiol/acrolein ratio of 1 (Figure 1e). It should also be noted that ^{1}H NMR analysis was conducted immediately upon mixing the copolymer with the acrolein solution. This suggests that the reaction between the sulfhydryl-functional copolymer and acrolein proceeds rapidly, which is consistent with the proposed thiol-Michael mechanism. For comparison, Figure 1f shows the reaction of acrolein with commercially procured dihydrolipoic acid as a control. Here a similar trend was observed where the area of the acrolein aldehyde resonance remained roughly constant as the thiol group concentration is increased while the vinyl resonance showed a concentration-dependent reduction in area. These results provide direct evidence that NPC 3 rapidly reacts with LPOx products potentially inactivating their neuro-destructive properties.

Based on the ability of NPC 3 to neutralize both ROS and LPOx products, we next evaluated the ability of the copolymer to protect neuron-like SH-SY5Y cells from these biochemical derangements. As shown in Figure 2a, cells treated with H_2O_2 began to show significant toxicity between 120 and 200 μM with a reduction in cell viability from 91 ± 2% to 29 ± 6% respectively and nearly complete cell death at 250 μM.

In comparison, cells preincubated with NPC 3 prior to H_2O_2 addition showed significantly higher viability over the same concentration range. Here nearly complete cell viability relative to untreated controls was observed even at a peroxide concentration of 200 μM. Some cell viability loss was observed at the highest H_2O_2 concentration tested (250 μM) however the polymer still provided significant improvements in relative to the untreated controls (i.e. 58 ± 0.4% vs. 9 ± 2%). Similarly, cells treated with acrolein alone over a concentration range of 2.5 to 25 μM showed a precipitous loss in viability from 100% viability at 2.5 μM to ~ 0 % viability at 12.5 μM (Figure 2b). In sharp contrast, incubation with NPC 3 provided essentially complete cell viability over the entire concentration range tested with only a modest reduction in cell viability to 94 ± 4% observed at 25 μM. These results taken together provide additional support for the neuroprotective properties of NPC 3. Further evidence supporting this hypothesis was provided by direct visualization of SH-SY5Y cell viability via confocal microscopy. Here SH-SY5Y cell were incubated with acrolein with or without the NPC 3 (0.3 mg mL^{-1}) for 18 hours. The cells were then stained with Hoescht nuclear stain (blue) and galectin-3 antibody (green) to label the cell membrane. As can be observed in Figure 2c, cells incubated with acrolein alone (25 μM) showed morphologies that were consistent with apoptosis while cells that were co-incubated with the copolymer (0.3 mg mL^{-1}) (Figure 2d) show morphologies that are similar to the untreated control (Figure 2e).

To evaluate how the protective effects of NPC 3 observed *in vitro* might translate to an animal model, dynamic contrast-enhanced magnetic resonance imaging (DCE-MRI)

was performed to assess brain uptake and accumulation in a CCI mouse model of TBI. Gadolinium (Gd)-based compounds are widely used to provide positive MRI contrast in both preclinical and clinical settings. [24] Gd was incorporated into NPC 3 in order to provide contrast enhancement and allow accumulation and retention of the copolymer in the brain to be followed. Here a polymerizable methacrylate monomer (ProbMer) containing a gadolinium-DOTA group (GdMA) was synthesized from cyclen in order to eliminate the need for costly and time-consuming post polymerization conjugation reactions. Characterization of contrast-enhancement at 9.4T showed T1 and T2 relaxivities of 3.05 $s^{-1}mM^{-1}$ and 8.21 $s^{-1}mM^{-1}$, respectively, and an r2/r1 of 2.69. These values suggest the viability of the compound for T1 enhancement as they are within range of Gd-DTPA, a clinically used agent, whose T1 relaxivity is 4.1 $s^{-1}mM^{-1}$ at 9.4T and r2/r1 is 1.12.[25] DCE-MRI was performed to estimate the volume transfer coefficient, K^{trans}, in the injured brain. K^{trans} describes the rate at which the contrast agent moves from the plasma into tissue and has been used previously to describe permeation across the disrupted blood-brain barrier (BBB) and in TBI mice.[25,26] K^{trans} mapping (Figure 3a,b) showed significantly higher permeation ($p = 0.0097$) in the injured region (mean $K^{trans} = 0.049$) compared with the contralateral hemisphere (mean $K^{trans} = 0.0026$). This observation of higher and more rapid uptake in the injured region combined with the ROS neutralization and cell viability data to suggest the potential for treatment of elevated ROS in the injured region with minimal off-target effects to the surrounding brain. Based on these data suggesting delivery to the brain, further *in vivo* testing was carried out to determine antioxidant effect in the injured brain.

NPC 3 was next tested in our CCI mice to evaluate the ability of the copolymer to reduce the spread of ROS following a CCI. Based on the MRI studies, which showed that NPC 3 passively accumulates and is retained in the brain injury following CCI (Figure 3a,b), mice were injected through the tail vein with 100 μL of NPC 3 at 2 mg/mL (8 mg/kg body weight) in DPBS immediately after impact. This provided a NPC 3 concentration of approximately 0.1 mg/mL in the blood. As a positive control, a well-known small antioxidant molecule, MnTMPyP, was employed.[27,28] MnTMPyP is a cell permeable SOD/catalase mimetic that possesses the catalytic activity of both enzymes. Here 500 μL of MnTMPyP at 1 mg/mL (20 mg/kg body weight) in DPBS was injected intraperitoneally immediately after impact to maximally reduce ROS levels at this dose.[29]

A DHE assay was then employed to observe the spread of ROS in the acute phase of the injury (4 h post-CCI). DHE becomes fluorescent when oxidized by ROS providing a convenient method for visualizing ROS levels in vivo. Since ROS are common signaling molecules in the brain and are produced as a byproduct of ATP production,[29] some DHE fluorescence is expected in the brain under physiological conditions. Therefore, the fluorescence intensity in the perilesional tissue was normalized to the contralateral hemisphere to reduce the variation of the base ROS in individual mice as well as to show the increase in ROS in the perilesional tissue. DHE fluorescence was highly increased in the perilesional area in CCI mice, which was reduced by treatments with MnTMPyP and NPC 3 (Figure 3c).

Quantifying these fluorescence levels across all animals (Figure 3d) revealed CCI mice had an approximately 43.9% increase in DHE fluorescence in the perilesional area as compared to contralateral brain (normalized DHE fluorescence of 1.439 ± 0.055). MnTMPyP significantly reduced DHE fluorescence to an 18.9% increase over contralateral brain (normalized DHE fluorescence of 1.189 ± 0.045). In comparison, NPC 3 provided nearly complete protected of the perilesional area, showing a 3.2% increase over contralateral brain (normalized DHE fluorescence of 1.032 ± 0.071). These results indicated that NPC 3 significantly reduced the spread of ROS in the acute phase of the injury compared to the untreated CCI mice. NPC 3 also seems to be more effective in reducing ROS compared to the small antioxidant molecule, MnTMPyP, which also significantly reduce the ROS compared to the untreated CCI mice. Thus, the *in vivo* DHE assay supports our in vitro findings that NPC 3 provides robust neuroprotective properties within 4 hours of NP injection in CCI mouse model of TBI.

Conclusions

A series of thiol-functionalized, water-soluble copolymers were synthesized for the targeted neutralization of ROS and LPOx. HRPO-H_2O_2 assays showed that NPC 3 was able to efficiently neutralize H_2O_2. The antioxidant properties of NPC 3 were further supported by RPE assays which demonstrated the ability of the copolymer to protect the ROS-sensitive protein from oxidation. Direct evidence for the ability of NPC 3 to covalently react with acrolein was provided by $_1$H NMR studies, which showed that the copolymer rapidly and quantitatively reacts with electron deficient LPOx. These results combined with in vitro cytotoxicity experiments conducted with SH-SY5Y differentiated neurons showed that NPC 3 provides substantial protection against acrolein. These findings were further supported by direct evaluation of cell morphology via confocal morphology where cells incubated with NPC 3 and acrolein showed morphologies similar to the untreated cells, while morphologies consistent with apoptosis were observed for the acrolein alone samples. Direct in vivo visualization of the theranostic copolymers via MRI demonstrated the passive accumulation and retention of these materials in a mouse model of TBI. Additionally, DHE assays showed that NPC 3 provides substantial reduction in the spread of biochemical derangements 4 hours in CCI mouse model of TBI. This suggests these materials may function well to reduce multiple mechanisms of secondary injury following TBI.

Supplementary Material

Refer to Web version on PubMed Central for supplementary material.

ACKNOWLEDGMENT

We acknowledge the Nano-Engineering Research Core facility supported by Nebraska Research Initiative fund for use of the confocal microscope. We thank Richard Watters for assistance with cell culture work. We thank Dr. Katie Shannon for assistance with optical imaging of cells.

Funding Sources

F.K. acknowledges support from the National Institute of Neurological Disorders and Stroke of the National Institutes of Health (R01NS109488). We would also like to acknowledge support from the Missouri S&T Center for Biomedical Research.

ABBREVIATIONS

CCR2	CC chemokine receptor 2
CCL2	CC chemokine ligand 2
CCR5	CC chemokine receptor 5
TLC	thin layer chromatography
TBI	Traumatic brain injury
ROS	reactive oxygen species
LPOx	lipid peroxidation product
4HNE	4-hydroxynonenal
LIPOMA	lipoic acid methacrylate
O950	polyethylene glycol monomethyl ether methacrylate
DOTA	2,2′2′′,2′′′-(1,4,7,10-Tetraazacyclododecane-1,4,7,10-tetrayl)tetraacetic acid
MRI	magnetic resonance imaging
NPCs	neuroprotective copolymers
RAFT	reversible addition-fragmentation chain transfer
CCI	controlled cortical impact
LA	lipoic acid
DHLA; $[M]_o$:$[CTA]_o$	dihydrolipoic acid; initial monomer to chain transfer agent ratio
$[CTA]_o$:$[I]_o$	initial chain transfer agent to initiator ratio
PBS	phosphate buffered saline
DLS	dynamic light scattering
HRPO	Horseradish peroxidase
RPE	R-phycoerythrin
ProbMer	polymerizable methacrylate monomer
DHE	dihydroethidium

REFERENCES

(1). Taylor CA; Bell JM; Breiding MJ; Xu L Traumatic Brain Injury-Related Emergency Department Visits, Hospitalizations, and Deaths - United States, 2007 and 2013. MMWR Surveill Summ 2017, 66, 1–16.

(2). McInnes K; Friesen CL; MacKenzie DE; Westwood DA; Boe SG Correction: Mild Traumatic Brain Injury (mTBI) and Chronic Cognitive Impairment: a Scoping Review. PLOS ONE 2019, 14, e0218423. [PubMed: 31185044]

(3). Mortezaee K; Khanlarkhani N; Beyer C; Zendedel A Inflammasome: Its Role in Traumatic Brain and Spinal Cord Injury. J Cell Physiol 2018, 233, 5160–5169. [PubMed: 29150951]

(4). Ladak AA; Enam SA; Ibrahim MT A Review of the Molecular Mechanisms of Traumatic Brain Injury. World Neurosurg 2019, 131, 126–132. [PubMed: 31301445]

(5). Liddelow SA; Guttenplan KA; Clarke LE; Bennett FC; Bohlen CJ; Schirmer L; Bennett ML; Münch AE; Chung W-S; Peterson TC; et al. Neurotoxic Reactive Astrocytes Are Induced by Activated Microglia. Nature 2017, 541, 481–487. [PubMed: 28099414]

(6). Hadass O; Tomlinson BN; Gooyit M; Chen S; Purdy JJ; Walker JM; Zhang C; Giritharan AB; Purnell W; Robinson CR; et al. Selective Inhibition of Matrix Metalloproteinase-9 Attenuates Secondary Damage Resulting From Severe Traumatic Brain Injury. PLOS ONE 2013, 8, e76904. [PubMed: 24194849]

(7). Mohamadpour M; Whitney K; Bergold PJ The Importance of Therapeutic Time Window in the Treatment of Traumatic Brain Injury. Front Neurosci 2019, 13, 07. [PubMed: 30728762]

(8). Di Pietro V; Yakoub KM; Caruso G; Lazzarino G; Signoretti S; Barbey AK; Tavazzi B; Lazzarino G; Belli A; Amorini AM Antioxidant Therapies in Traumatic Brain Injury. Antioxidants (Basel) 2020, 9, 260.

(9). Hall ED; Wang JA; Miller DM; Cebak JE; Hill RL Newer Pharmacological Approaches for Antioxidant Neuroprotection in Traumatic Brain Injury. Neuropharmacology 2019, 145, 247–258. [PubMed: 30086292]

(10). Gruenbaum SE; Zlotnik A; Gruenbaum BF; Hersey D; Bilotta F Pharmacologic Neuroprotection for Functional Outcomes After Traumatic Brain Injury: a Systematic Review of the Clinical Literature. CNS Drugs 2016, 30, 791–806. [PubMed: 27339615]

(11). Reddy MK; Labhasetwar V Nanoparticle-Mediated Delivery of Superoxide Dismutase to the Brain: an Effective Strategy to Reduce Ischemia-Reperfusion Injury. FASEB J. 2009, 23, 1384–1395. [PubMed: 19124559]

(12). Liu TH; Beckman JS; Freeman BA; Hogan EL; Hsu CY Polyethylene Glycol-Conjugated Superoxide Dismutase and Catalase Reduce Ischemic Brain Injury. Am J Physiol 1989, 256, H589–H593. [PubMed: 2492771]

(13). Marshall LF; Maas AI; Marshall SB; Bricolo A; Fearnside M; Iannotti F; Klauber MR; Lagarrigue J; Lobato R; Persson L; et al. A Multicenter Trial on the Efficacy of Using Tirilazad Mesylate in Cases of Head Injury. J Neurosurg 1998, 89, 519–525. [PubMed: 9761043]

(14). Tarudji AW; Gee CC; Romereim SM; Convertine AJ; Kievit FM Antioxidant Thioether Core-Crosslinked Nanoparticles Prevent the Bilateral Spread of Secondary Injury to Protect Spatial Learning and Memory in a Controlled Cortical Impact Mouse Model of Traumatic Brain Injury. Biomaterials 2021, 272, 120766. [PubMed: 33819812]

(15). Yoo D; Magsam AW; Kelly AM; Stayton PS; Kievit FM; Convertine AJ Core-Cross-Linked Nanoparticles Reduce Neuroinflammation and Improve Outcome in a Mouse Model of Traumatic Brain Injury. ACS nano 2017, 11, 8600–8611. [PubMed: 28783305]

(16). Xu J; Ypma M; Chiarelli PA; Park J; Ellenbogen RG; Stayton PS; Mourad PD; Lee D; Convertine AJ; Kievit FM Theranostic Oxygen Reactive Polymers for Treatment of Traumatic Brain Injury. Advanced Functional Materials 2016, 26, 4124–4133.

(17). Ferrari R; Ceconi C; Curello S; Cargnoni A; Alfieri O; Pardini A; Marzollo P; Visioli O Oxygen Free Radicals and Myocardial Damage: Protective Role of Thiol-Containing Agents. Am J Med 1991, 91, 95S–105S.

(18). Chan JW; Hoyle CE; Lowe AB; Bowman M Nucleophile-Initiated Thiol-Michael Reactions: Effect of Organocatalyst, Thiol, and Ene. Biomacromolecules 2010, 43, 6381–6388.

(19). Packer L; Witt EH; Tritschler HJ Alpha-Lipoic Acid as a Biological Antioxidant. Free Radic Biol Med 1995, 19, 227–250. [PubMed: 7649494]

(20). Schönheit K; Gille L; Nohl H Effect of Alpha-Lipoic Acid and Dihydrolipoic Acid on Ischemia/Reperfusion Injury of the Heart and Heart Mitochondria. Biochim. Biophys. Acta 1995, 1271, 335–342. [PubMed: 7605800]

(21). Roy D; Berguig GY; Ghosn B; Lane DD; Braswell S; Stayton PS; Convertine AJ Synthesis and Characterization of Transferrin-Targeted Chemotherapeutic Delivery Systems Prepared via RAFT Copolymerization of High Molecular Weight PEG Macromonomers. Polymer Chemistry 2014, 5, 1791–1799. [PubMed: 25221630]

(22). Das D; Srinivasan S; Kelly AM; Chiu DY; Daugherty BK; Ratner DM; Stayton PS; Convertine AJ RAFT Polymerization of Ciprofloxacin Prodrug Monomers for the Controlled Intracellular Delivery of Antibiotics. Polymer Chemistry 2016, 7, 826–837.

(23). Das D; Chen J; Srinivasan S; Kelly AM; Lee B; Son H-N; Radella F; West TE; Ratner DM; Convertine AJ; et al. Synthetic Macromolecular Antibiotic Platform for Inhalable Therapy Against Aerosolized Intracellular Alveolar Infections. Mol. Pharm. 2017, 14, 1988–1997. [PubMed: 28394614]

(24). Bellin M-F MR Contrast Agents, the Old and the New. Eur J Radiol 2006, 60, 314–323. [PubMed: 17005349]

(25). Miller HA; Magsam AW; Tarudji AW; Romanova S; Weber L; Gee CC; Madsen GL; Bronich TK; Kievit FM Evaluating Differential Nanoparticle Accumulation and Retention Kinetics in a Mouse Model of Traumatic Brain Injury via Ktrans Mapping with MRI. Sci Rep 2019, 9, 16099–14. [PubMed: 31695100]

(26). Montagne A; Barnes SR; Sweeney MD; Halliday MR; Sagare AP; Zhao Z; Toga AW; Jacobs RE; Liu CY; Amezcua L; et al. Blood-Brain Barrier Breakdown in the Aging Human Hippocampus. Neuron 2015, 85, 296–302. [PubMed: 25611508]

(27). Wang X; Sun D; Hu Y; Xu X; Jiang W; Shang H; Cui D The Roles of Oxidative Stress and Beclin-1 in the Autophagosome Clearance Impairment Triggered by Cardiac Arrest. Free Radic Biol Med 2019, 136, 87–95. [PubMed: 30951836]

(28). Nair AB; Jacob S A Simple Practice Guide for Dose Conversion Between Animals and Human. J Basic Clin Pharm 2016, 7, 27–31. [PubMed: 27057123]

(29). Beckhauser TF; Francis-Oliveira J; De Pasquale R Reactive Oxygen Species: Physiological and Physiopathological Effects on Synaptic Plasticity. J Exp Neurosci 2016, 10, 23–48. [PubMed: 27625575]

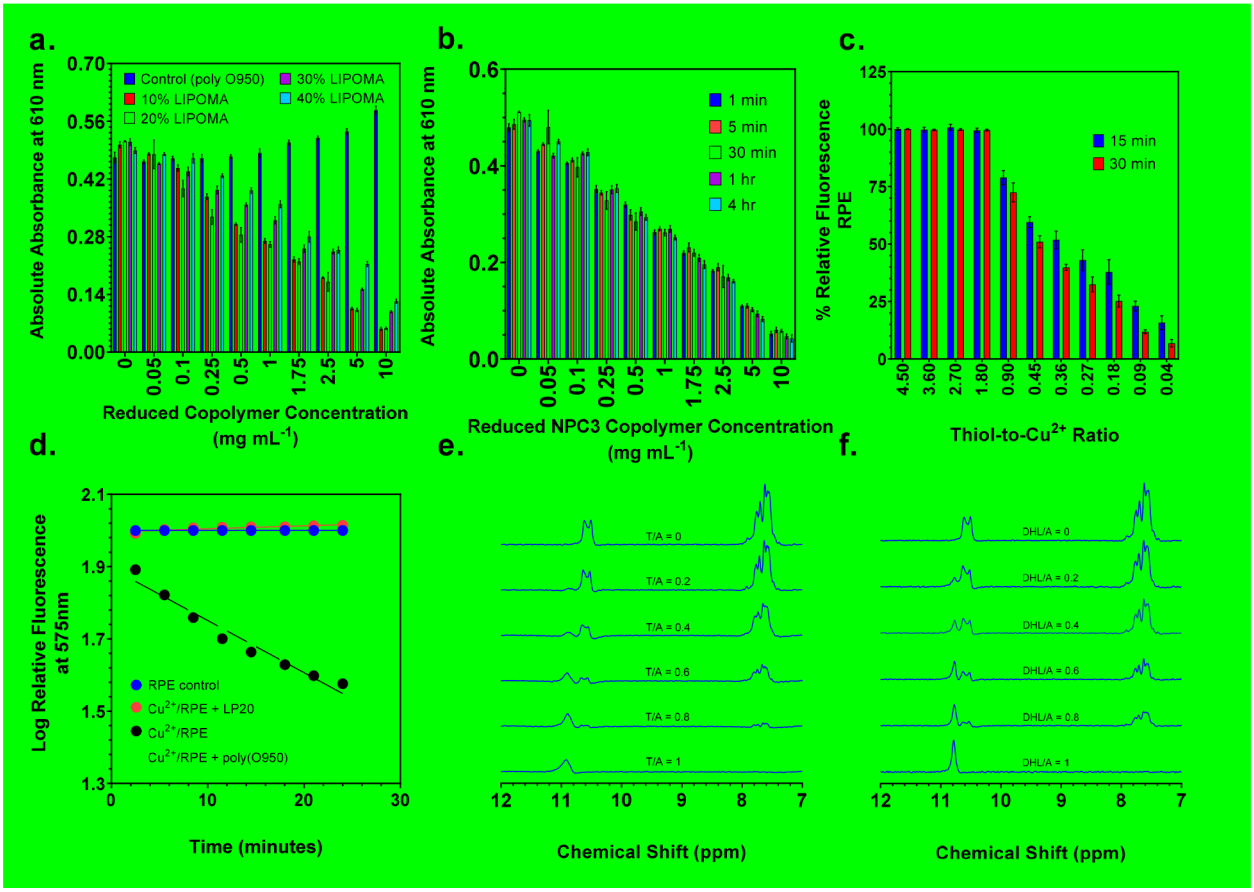

Figure 1.

(a) Absolute absorbance values as a function of NPC composition and concentration in HRPO assays. (b) Reduction in absolute absorbance values as a function of incubation time and concentration for NPC 3 copolymer in HRPO assays. (c) RPE protein analysis of polymer induced neutralization of free radicals produced by the Fenton reaction between ascorbic acid and a Cu2+, illustrated by reduction in relative fluorescence values as a function of decreasing thiol/Cu^{2+} ratio. (d) Relative fluorescence as a function of time for RPE incubated with and without reduced NPC 3 and the negative control poly(O950) polymer. ^{1}H NMR studies conducted in D_2O show thiol groups react with LPOx alkenes via thiol-Michael reactions resulting in the formation of thioether adducts between acrolein and (e) dihydrolipoic acid sodium salt or (f) NPC 3 copolymer. Three samples (n=3) were run for each concentration in HRPO and RPE assays. Average and standard deviation were determined for each concentration from the three samples.

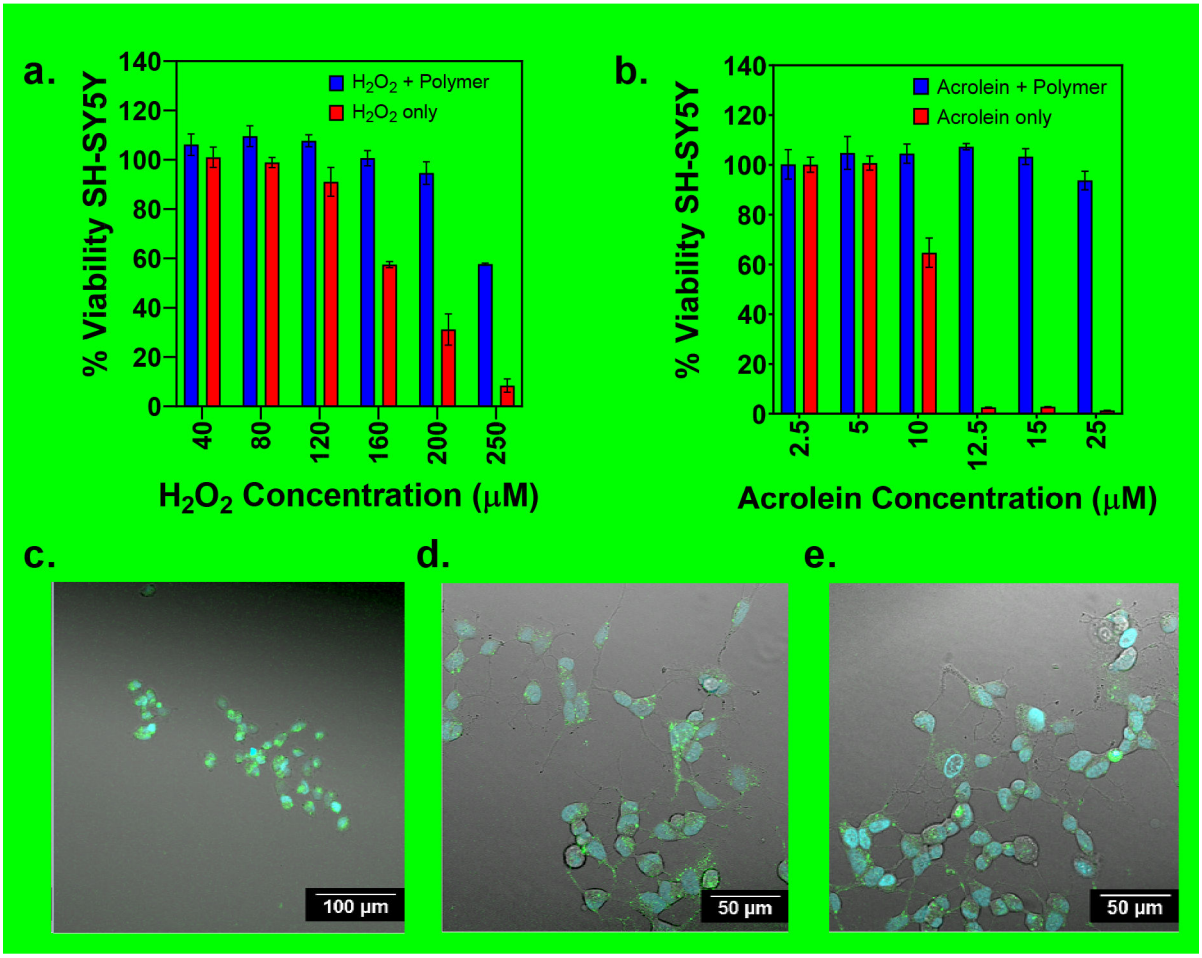

Figure 2.

% SH-SY5Y cell viability for neuroblastoma differentiated cells as a function of increasing (a) peroxide and (b) acrolein concentration with and without reduced poly(LIPOPMA-co-O950) (0.3 mg/mL). Cells were either left untreated, treated with acrolein or treated with polymer and acrolein prior to determination of cell viability via MTT. Optical microscopy images were taken for (c) cells treated with acrolein, (d) cells incubated with NPC 3 copolymer prior to acrolein addition, and (e) untreated cells. Three trials (n=3) were run at each concentration in triplicate for MTT viability protection assays. Standard deviation for each concentration were determined using the averages of the three trials.

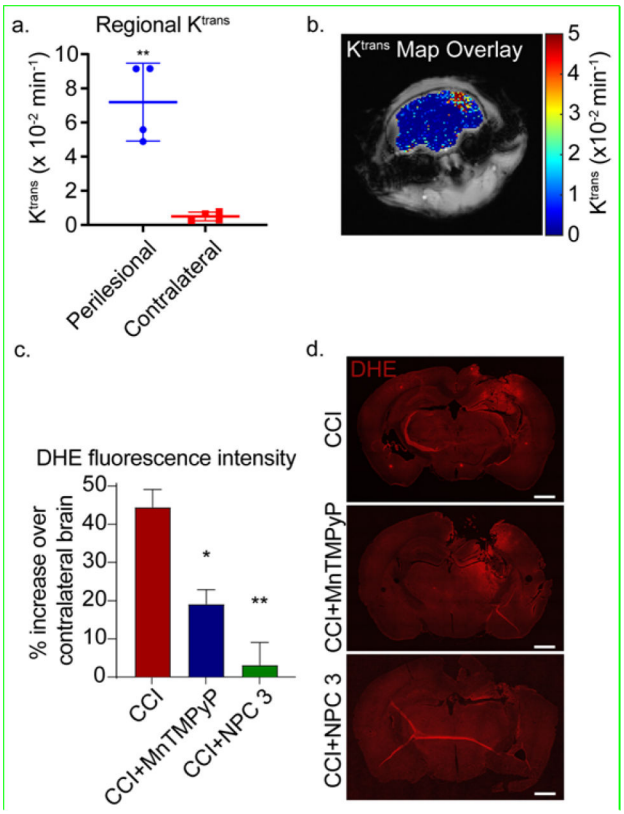

Figure 3.

(a-b) *In vivo* DCE-MRI and K^{trans} mapping of mice 3 h post-injury. (a) Significantly higher K^{trans} was observed in the ipsilateral region compared with the contralateral ($p = 0.0097$) as determined by paired t-test. (b) The K^{trans} map shows higher permeability (red) corresponds with the ipsilateral region (right side of the brain in the image) while lower values are observed in the contralateral hemisphere. (c-d) *In vivo* DHE staining of the brains at 4 h post-injury. c) The DHE fluorescence mean intensity at the perilesional normalized to the contralateral hemisphere. Data are shown as mean ± SEM with n = 3 for each treatment group; 1.439 ± 0.055 for untreated CCI mice, 1.189 ± 0.045 for MnTMPyP treated CCI mice, and 1.032 ± 0.071 for NPC 3 treated CCI mice. * indicates a statistical difference compared to control with one and two symbols indicating $p < 0.05$ and $p < 0.01$, respectively, as determined by one-way ANOVA and Tukey's post hoc test. (d) Representative images of the DHE staining of the untreated CCI mice, MnTMPyP treated CCI mice, and NPC 3 treated CCI mice. The scale bar is 1000 μm.

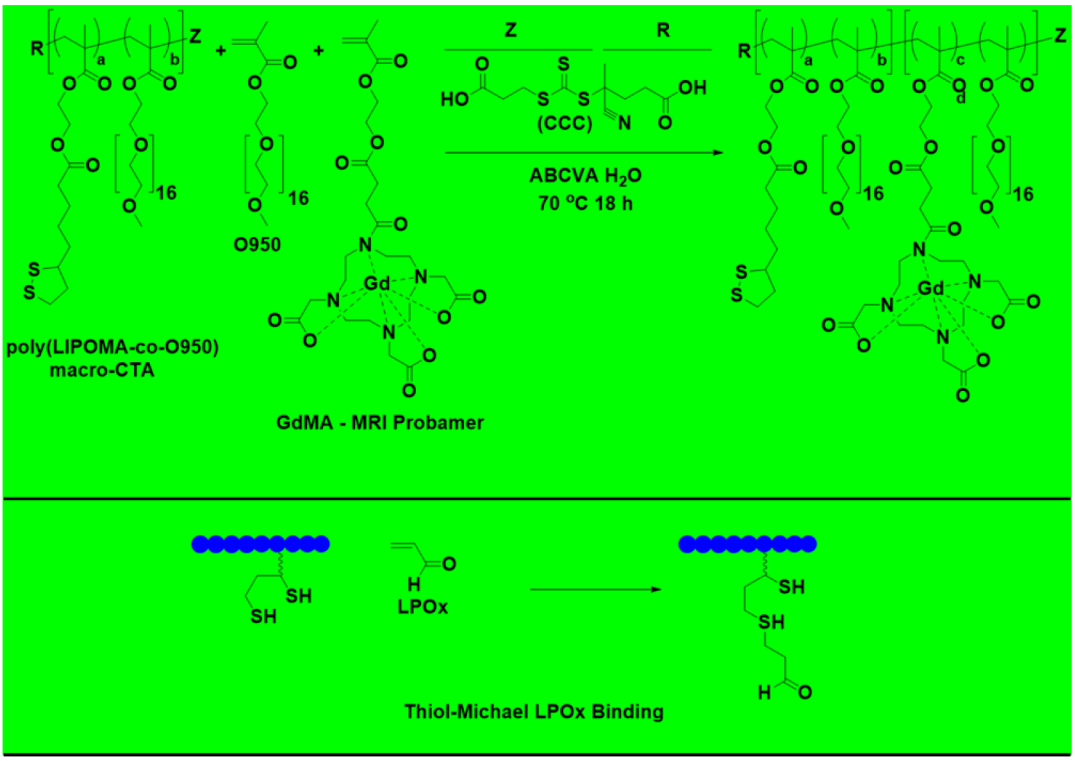

Scheme 1.

Synthetic strategy for the RAFT synthesis of neuroprotective copolymers (NPCs) blocked with MRI contrast GdMA using isolated LIPOMA-co-O950 NPC series macro CTA and proposed mechanism for covalent neutralization of lipid peroxidation products. Disulfide bonds were reduced to thiols by reacting purified block copolymer $NaBH_4$ in DMAc. LIPOMA-co-O950 NPC series macro CTAs without GdMA were directly reduced with $NaBH_4$, purified, and tested. All LIPOMA-co-O950 macro CTAs were RAFT synthesized in DMAc at 70°C for 24 hrs using CCC and ABCVA.

Table 1.

Molecular weight and composition data for poly(LIPOMA-co-O950) copolymers prepare by RAFT copolymerization.

NPC	Target wt. % LIPOMA	M_n Theory (Da)	M_n Exp. (Da)	Molar Mass Dispersity (Đ)	D_H (nm)
1	0	24 000	24 000	1.17	7.0
2	10	20 500	28 000	1.18	5.0
3	20	17 400	26 700	1.25	9.0
4	30	15 300	28 100	1.28	14
5	40	13 700	29 700	1.35	14
6	50	12 400	27 900	1.40	19